

## Full Paper

## Development and Scale-up of Continuous Electrocatalytic Hydrogenation of Functionalized Nitroarenes, Nitriles and Unsaturated Aldehydes

Jonathan D Egbert, Edwin C. Thomsen, Stacy A. O'Neill-Slawecki, Douglas M Mans, David C. Leitch, Lee J. Edwards, Charles E Wade, and Robert S. Weber

*Org. Process Res. Dev.*, **Just Accepted Manuscript** • DOI: 10.1021/acs.oprd.8b00379 • Publication Date (Web): 08 Jul 2019

Downloaded from pubs.acs.org on July 12, 2019

### Just Accepted

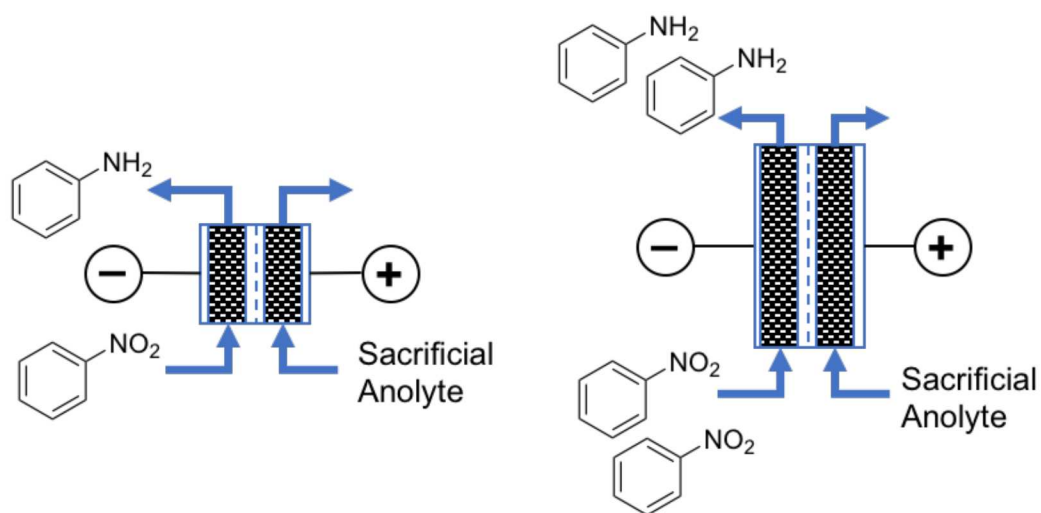
"Just Accepted" manuscripts have been peer-reviewed and accepted for publication. They are posted online prior to technical editing, formatting for publication and author proofing. The American Chemical Society provides "Just Accepted" as a service to the research community to expedite the dissemination of scientific material as soon as possible after acceptance. "Just Accepted" manuscripts appear in full in PDF format accompanied by an HTML abstract. "Just Accepted" manuscripts have been fully peer reviewed, but should not be considered the official version of record. They are citable by the Digital Object Identifier (DOI®). "Just Accepted" is an optional service offered to authors. Therefore, the "Just Accepted" Web site may not include all articles that will be published in the journal. After a manuscript is technically edited and formatted, it will be removed from the "Just Accepted" Web site and published as an ASAP article. Note that technical editing may introduce minor changes to the manuscript text and/or graphics which could affect content, and all legal disclaimers and ethical guidelines that apply to the journal pertain. ACS cannot be held responsible for errors or consequences arising from the use of information contained in these "Just Accepted" manuscripts.

# Development and Scale-up of Continuous Electrocatalytic Hydrogenation of Functionalized Nitro arenes, Nitriles and Unsaturated Aldehydes

Jonathan D. Egbert<sup>1</sup>, Edwin C. Thomsen<sup>1</sup>, Stacy A. O'Neill-Slawecki<sup>2</sup>, Douglas M. Mans<sup>2†</sup>,  
David C. Leitch<sup>2+</sup>, Lee J. Edwards<sup>3</sup>, Charles E. Wade<sup>3</sup> and Robert S. Weber<sup>\*1</sup>

<sup>1</sup>Institute for Integrated Catalysis, PNNL, Richland, WA 99352 (USA), <sup>2</sup>GSK, Advanced  
Manufacturing Technologies, King of Prussia, PA 19406 (USA), <sup>3</sup>GSK, API Chemistry,  
Stevenage, Hertfordshire, SG1 2NY, (UK), current address: <sup>†</sup>Environmental Molecular Sciences  
Laboratory, PNNL, Richland, WA 99352, USA; <sup>+</sup>Department of Chemistry, University of  
Victoria, PO Box 1700 Stn CSC, Victoria BC V8W2Y2, Canada

For Table of Contents only



ABSTRACT Electrolysis flow reactors based on the filter-press architecture of redox flow batteries have proven to be effective and scalable towards the production of commercially relevant, pharmaceutical quantities of anilines (>500 kg/year) from halogen-, hydroxyl-, and carbonyl-substituted nitroarenes. Turbulent flow through the carbon felts on which the catalysts were supported facilitated scaling towards production levels because it conferred on the reactors scale-independent, plug flow-like residence time distributions and high mass transfer coefficients. Equipping the cells with micro-reference electrodes made it possible to transfer reaction conditions first developed in batch systems to the continuous flow reactors. The catalysts prepared by incipient wetness impregnation of metal salts into lightly oxidized carbon felt supports were readily generalizable.

Keywords: electrosynthesis, reduction, anilines hydrodeoxygenation of nitro arenes, hydrogenation, flow chemistry

## Introduction

Despite more than 100 years of promise<sup>1-7</sup> for the selective, safe, and “green” conversions<sup>8-10</sup> of organic compounds, fewer than ~0.3% ( $\approx 14/4500$ ) of the processes described in papers published in ORGANIC PROCESS RESEARCH AND DEVELOPMENT exploit electrochemical routes and only one of those has been reported to have been scaled from lab to pilot operation (Table 1). We believe that several issues contribute to the disparity between promise and implementation: 1) the unfamiliarity of both synthetic organic chemists and their engineering counterparts with electrochemical transformations,<sup>2</sup> 2) lack of readily scaled reactors,<sup>11</sup> 3) difficulty in transferring kinetics measurements from bench to production, and 4) the effort required to identify and prepare customized electrocatalysts. The advent of commercial, bench-scale electrochemical

1  
2  
3 flow reactors (e.g. IKA,<sup>12</sup> CTech,<sup>13</sup> and The Fuel Cell Store<sup>14</sup>) help address the first issue but not  
4  
5 the other impediments.  
6

7  
8 Here we describe an electrochemical flow reactor (i.e., a reactor incorporating continuous flow  
9  
10 of the electrolytes), along with its easily prepared catalysts, that were designed to be scalable to  
11  
12 at least the throughput required for the production of active pharmaceutical intermediates. The  
13  
14 breadth of the selection of reactions presented below was enabled by the readily varied reaction  
15  
16 conditions (applied potential, residence time) and the readily varied catalyst compositions. The  
17  
18 selection, however, is only intended to be illustrative and evocative, and does not bear on the use  
19  
20 of electrochemistry for separations, waste remediation or the preparation of commodity products  
21  
22 or intermediates.<sup>15</sup> Thanks to the use of a semi-structured catalyst support (carbon felt), which  
23  
24 also served as the cathode, the rheology and transport characteristics of the reactor proved to be  
25  
26 similar across a 20-fold increase in reactor volume (10 cm<sup>2</sup> –200 cm<sup>2</sup> at a half-cell depth of 5  
27  
28 mm). Stacking less than 20 of the largest reactors promises 0.5 T/y production of an aryl amine  
29  
30 via the 6-electron reduction of the analogous nitro arenes, with the caveat that improvements  
31  
32 would be required in catalyst stability or a strategy for replacement.  
33  
34  
35  
36  
37  
38  
39  
40  
41  
42  
43  
44  
45  
46  
47  
48  
49  
50  
51  
52  
53  
54  
55  
56  
57  
58  
59  
60

Table 1. Electrochemistry-themed, primary articles published in Organic Process Research and Development since the inception of the journal.

Year	Reaction	Focus	Scale and conditions <sup>a</sup>
2002	Reduction of an ester to an exo-methylene <sup>16,17</sup>	Scale up	Lab: g-scale, Electrosyn MP flow cell (0.02 m <sup>2</sup> ) Pilot: kg-scale, ICI FM-21, 0.42 m <sup>2</sup> Applied potential: ~6 V
2004	Oxidation of NADH <sup>18</sup>	Proof of concept and modeling	Analytical (mM) Applied half-cell potential < 0.6 V
	Reduction of maleic acid <sup>18,19</sup>	Effect of process conditions	Lab, ICI FM-01, 64 cm <sup>2</sup> electrode Applied potential: 2-5 V
2005	Oxidation of a protected piperidine <i>en route</i> to a ketone <sup>20</sup>	Synthetic chemistry	Lab (50 mL beaker) controlled current operation
2008	Oxidative iodination of aromatics <sup>21</sup>	Synthetic chemistry	Lab (g scale in an H-cell and with a microflow mixer) Applied potential not reported
2014	Reductive removal of a protecting group <sup>22</sup>	Synthetic chemistry	Lab (<90 μmol/h) Applied potential not reported
2015	Dehydrogenative Methoxylation <sup>23</sup>	Reactor design	Lab (1-24 g product; 8-16 mL/min) controlled current operation
	Dehalogenation of strained rings <sup>24</sup>	Synthetic chemistry and Reactor design	Lab (Batch: 2 L, 25 g; Flow: 0.5 to 1.5 mL/min) Applied potential: 13 V
2016	Various <sup>25</sup> (cross-coupling, dehalogenation, deoxygenation, etc).	High throughput catalyst screening	Analytical (< 10 mL cell volume, ~1 mm <sup>2</sup> electrode) controlled current operation
	Reduction of CO <sub>2</sub> <sup>26</sup>	Quantum chemical modeling	—
2017	Synthesis of nitriles from aldoximes <sup>27</sup>	Synthetic chemistry and process optimization	Lab (7.5-15 mL/h, 12 cm <sup>2</sup> electrode) controlled current operation
2018	Oxidation of an alcohol <sup>28</sup>	Catalyst synthesis	Lab (batch reactor, 80-120 mL)
	Electrocatalytic hydrogenation <sup>29</sup>	Synthetic chemistry and activity of platinum group metals	Lab (60 mL batch reactor; flow reactor: 2 mL/min) controlled current
2019	Electrocatalytic hydrogenation of furfural <sup>30</sup>	Flow microreactor	Lab (4.5 mL/h); controlled voltage

- a) The applied potentials were those gleaned from the associated literature. We infer that they were cell or stack potentials, not half-cell potentials. Unfortunately, the literature does not report that parameter consistently, or even carefully; the situation is tantamount to heating a reactor to achieve a specified reaction rate but then not reporting the temperature.

## Design strategy

To illustrate the input power and material flow through a continuous electrochemical process employed for the production of a fine or specialty chemical, consider the example of a flow

electrolysis cell operating at 1 kW that effects a  $4e^-$ -conversion of a 100 g/mol substrate at a cell potential,  $E_{cell} = 1.5$  V will produce about 5 T per year of product (eq. 1):

$$\frac{1000 \text{ VA} \times 100 \frac{\text{g}}{\text{mol}} \times 3.15 \times 10^7 \text{ s/y}}{1.5 \text{ V} \times \frac{4 \times 96485 \text{ C}}{\text{mol}}} = 5.4 \text{ T/y} \quad \text{eq. 1}$$

For reference, redox flow batteries, which are just flow electrolysis cells, are now routinely sized for delivering >100 MW of power.<sup>31</sup> Because prior experience at PNNL had demonstrated the scalability of filter-press redox flow batteries<sup>32</sup> (Figure 1), we repurposed the architecture here.

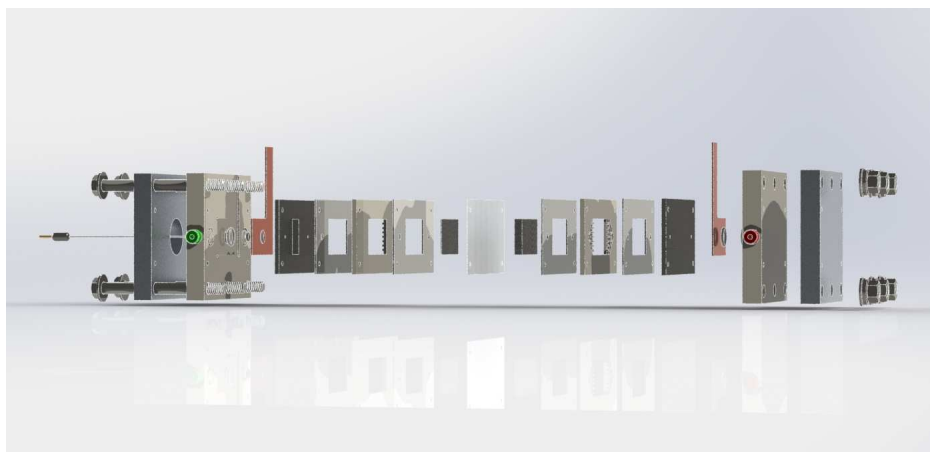


Figure 1. Exploded view of the geometry of a single stage (1 anode, 1 cathode) flow electrolysis cell based on the PNNL design for a redox flow battery, showing (outward from the center): Nafion® separator, carbon felt electrodes, PEEK spacers, graphite flow distributors, copper electrodes, PEEK insulators, thrust plates and, on the left, the micro reference electrode.

We constructed three sizes of the reactors (Figure 2), equipped with ports for small reference electrodes, however we employed reference electrodes only in a few instances noted below. The rectangular catalyst cavities varied in volume from 5 cm<sup>3</sup> to 100 cm<sup>3</sup>, all having the same cross-sectional aspects (Table 2).



Figure 2. Three sizes of flow electrolysis cells.

Table 2. Dimensions of the catalyst cavities in the three test cells and their Reynolds numbers at a residence time typical of the electrolysis experiments.

Cell	W/cm	H/cm	D/cm	$d_c \equiv 2DW/(D+W)$	$L_c \equiv H/d_c$	Re at $\tau = 300s$
Small	2.4	4.2	0.5	0.83	5.1	0.7
Medium	5.7	10.0	0.5	0.92	10.9	1.8
Large	10.7	18.7	0.5	0.95	19.6	3.5

W-width, H-height, D-depth, Re-Reynolds number ( $Re = u d_c \rho / \mu$ ),  $\tau$ -residence time

## Experimental Section

**Materials.** The cells were constructed from stainless steel (end plates), PEEK (frame), copper (current collectors), graphite (flow field), Teflon (gaskets), and Nafion® 117 (membrane). The electrolytes were delivered from their reservoirs through PEEK tubing using gear pumps equipped with graphite impellers. The anode was a piece of Pt/C paper, 2 mg<sub>Pt</sub>/cm<sup>2</sup> (The Fuel Cell Store).

The cathodes (Table 3) were prepared, as described previously,<sup>29,33</sup> by incipient wetness impregnation of a graphite felt (0.6 cm thick, Alfa-Aesar #43200) that had been previously rendered hydrophilic by mild oxidation in air. The selected metal salt (each obtained from Sigma Aldrich) were dissolved in the 11 mL/g of water that just wet the support to achieve the desired metal loading. The impregnated felts (~3 g pieces) were then dried and calcined in flowing,



diluted air (~1 mol% O<sub>2</sub>). We targeted, and achieved, metal loadings in the range of 1-4 wt% as determined by ICP (Galbraith Labs). The cathodes compressed to 5 mm when mounted in the cells. The Cu/C/membrane electrocatalyst was kindly prepared for us by the research group of Prof. Eugene Smotkin using a catalyst ink made from carbon black impregnated with copper(II)acetate mixed with a Nafion<sup>®</sup> ionomer solution that was, in turn, painted and dried onto a Nafion<sup>®</sup> 117 membrane, according to the usual practice in that laboratory.<sup>34</sup>

Table 3. Catalysts and their test reactions.

Catalyst	Precursor	Test Reactions
Fe/C felt	Fe(II)acetylacetonate	Hydrodeoxygenation of nitrobenzene
Co/C felt	Co(II)acetate	Hydrogenation of benzonitrile
Cu/C felt	Cu(II)acetate	Hydrodeoxygenation of nitrobenzene, 1-chloro-2-methyl-3-nitrobenzene and methyl 3-nitrobenzoate; Hydrogenation of cinnamaldehyde
Cu/C/Membrane	Cu(II)acetate	Hydrodeoxygenation of methyl 3-nitrobenzoate
Ag/C felt	Ag(I)acetate	Hydrogenation of cinnamaldehyde
Pd/C felt	Pd(II)acetate	Hydrodeoxygenation of 1-chloro-2-methyl-3-nitrobenzene

The catholytes (Table 4) consisted of the selected substrate at the indicated concentration plus 5wt% acetic acid dissolved in methanol:H<sub>2</sub>O (80:20 by weight) solution. The anolyte consisted of 1 M KOH (Sigma Aldrich, anhydrous ≥99%) dissolved in the methanol:H<sub>2</sub>O solution (4:1 by weight) solution.

Table 4. Composition of the test solutions

Test reaction	Catholyte
Hydrodeoxygenation of nitro arenes Hydrogenation of cinnamaldehyde	Indicated concentration of substrate dissolved in acetic acid diluted to 470 mM with MeOH/H <sub>2</sub> O (4:1)

Hydrogenation of benzonitrile	100 mM benzonitrile in a solution of THF containing 5 wt% and acetic acid (400 mM) 100 mM benzonitrile in a solution of methanol containing 10wt% water and 400 mM acetic acid
-------------------------------	-----------------------------------------------------------------------------------------------------------------------------------------------------------------------------------

**Flow visualization.** To visualize the flow in the electrolysis cells, we replaced one of the endplates with a glass window and followed the flow of Rhodamine G, a fluorescent dye injected into the cathode compartment. The volumetric flow rate of the fluid (water) was set at 1 mL/min, which corresponded to a Reynolds number for the empty channel of 0.7 (Table 2)

**Residence time distribution.** We measured the current response of the cell when a bolus of electrolyte was injected into the cathode feed by momentarily switching the inlet from a non-conductive fluid (water) to a conductive fluid (the electrolyte without substrate). The results were converted to dimensionless time,  $\theta = t/\tau$ , by dividing the elapsed time by the hydraulic residence times of the cells ( $\tau$  = cell volume/volumetric flow rate of the fluid) and then normalizing the curves to unit area. The duration of each bolus was approximately 120 seconds. The residence time distributions,  $E(\theta)$ , were modeled by fitting them to the convolution of a square pulse,  $Sq$ , of width,  $w$ , centered at time,  $\theta = c$ , and the analytical form of a plug flow reactor with axial dispersion,<sup>35</sup> characterized by an axial Peclet number,  $Pe_a$  (equation 2):

$$E(\theta) = \int_0^\infty \left( \frac{Pe_a}{4\pi\theta} \right)^{1/2} \exp \left( -\frac{(1-\theta)^2 Pe_a}{4\theta} \right) \times Sq(t - \theta, w, c) dt \quad \text{eq. 2}$$

We used the Matlab routine,<sup>36</sup> `lsqcurvefit`, to optimize the fit of the measured residence time distributions to the calculated  $E(\theta)$  by varying the three parameters,  $Pe_a$ ,  $w$  and  $c$  (the pulsewidth and midpoint were varied because the lag times were not known for the system).

**Mass transfer.** We used linear sweep voltammetry of ferricyanide reduction<sup>37</sup> to estimate the mass transfer coefficient for transporting species to and from the felt cathode as a function of the

flow rate of the electrolyte through the electrode, expressed as the dependence of the Sherwood number,  $Sh \equiv k_m d_e/D$ , on the Reynolds number,  $Re$ . In the transport limited regime (i.e. at cathodic enough overpotential, here,  $E_{\text{cell}} < -1.5$  V), the current,  $I$ , is proportional to the product of the exposed surface area of the electrode,  $A$ , the concentration of the reducible ion,  $C_0$ , with the mass transfer coefficient,  $k_m$  being the constant of proportionality (eq. 3):

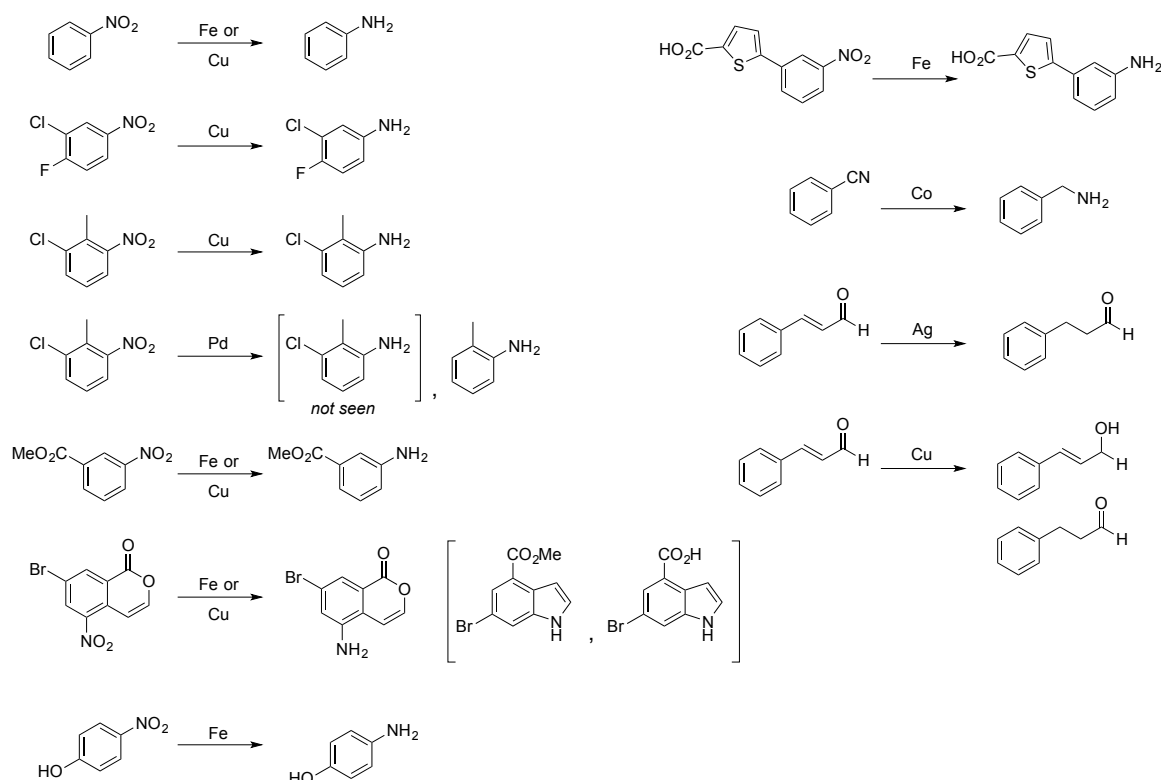
$$I = k_m A C_0 \quad \text{eq. 3}$$

In our experiments, the surface area of the felt was about  $1 \text{ m}^2/\text{g}$ , i.e., about as low as we could measure using nitrogen physisorption (Micromeritics, ASAP 2020; the results are consistent with the geometry of the fibers comprising the felt as imaged by scanning electron microscopy). The mass of the felt was 0.484 g and the inlet concentration of potassium ferricyanide was 1.18 mM dissolved in a 38.6 mM aqueous solution of potassium carbonate; the anolyte was 1 M potassium hydroxide. We used a value of  $0.740 \times 10^{-5} \text{ cm}^2/\text{s}$  for the diffusion coefficient,  $D$ , of the ferricyanide ions.<sup>38</sup>

**Reaction Kinetics.** We measured the conversion of the substrates (Scheme 1) catalyzed by the selected metals as a function of residence times in the range of 150 to 450 s, applied cell potentials (in the range of -0.1 to -1.5 V), electrolyte, at several concentrations and temperatures. Gear pumps equipped with graphite impellers were used to meter the flow of the electrolytes. The temperature was controlled by inserting the whole cell in an oven. The alternative, heating anolyte and using the cell as a heat exchanger to heat the catholyte, incurred unacceptably large thermal losses at the small flow rates we studied. Inlet and exiting concentrations were quantified using an Agilent GC/MS (30 m  $\times$  0.25 mm column of RXI-5Sil MS) where the temperature of the GC column was ramped to 85 °C, held for 2 min, then ramped at 10 °C/min to 170 °C where it was held for 2 min.

While we were content with the performance of the graphite felt as the catalyst support for the cathode catalyst, we also tested supporting the catalyst directly on the intercell membrane. Supporting the metal directly on the membrane, each side of which contacts a current conductor, is the preferred architecture for hydrogen fuel cells, because the configuration should provide a higher flux of protons from the anode catalyst to the cathode catalyst. However, the immediate environment of the electrocatalyst in that case is very hydrophilic, which may impede the approach of the lipophilic substrates tested here. The hydrodeoxygenation of 1-chloro-2-methyl-3-nitrobenzene was used to compare the performance of a Cu cathode supported on the Nafion<sup>®</sup> membrane with a similar loading of Cu supported on the felt.

**Applied potential and Sign Convention.** The potential across the electrolysis cell was controlled by connecting the reference electrode to the cathode and setting the potentiostat to a negative voltage. We indicate that the experiments were operated at a negative cell potential,  $E_{cell}$ , to emphasize that we focused on the cathodic reactions.



Scheme 1. The studied reactions and their catalysts. The catalysts were the indicated metal supported on graphitic carbon felt.

**Scale-up.** As an intermediate stage in scaling from bench to production, we ran the hydrodeoxygenation of 1-chloro-2-methyl-3-nitrobenzene in the small reactor and in two medium sized reactors connected in parallel (Figure 3) to achieve a higher conversion and a higher throughput by operation at twice the residence time and an order of magnitude (factor of 12) higher flow rate. The cells were run at constant potential. We did not accurately quantify either the yields of products or the Faradaic efficiencies of the conversions because our intent was rather to survey a range of reactions rather than optimize conditions with respect to conversion or selectivity. Even so, we were gratified to observe moderate conversions and high product selectivities (Scheme 2).

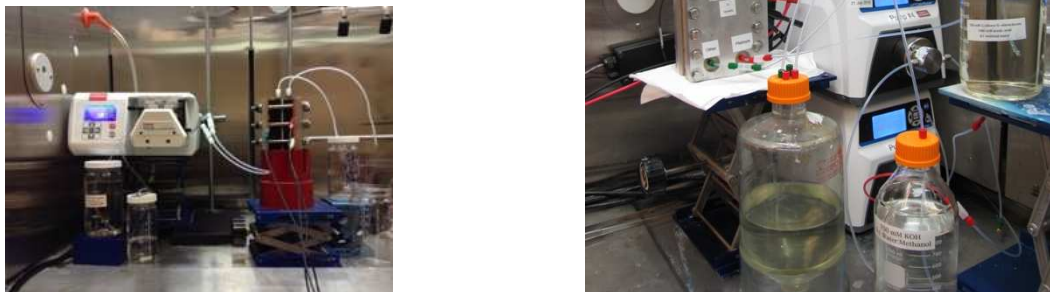


Figure 3. Installation of the small reactor and a pair of the medium scale, single stage reactors plumbed in parallel. Each reactor contains a single cathode compartment and a single anode compartment. These cells ran potentiostatically and did not include a reference electrode.

## Results and Discussion

**Flow visualization.** When the fluid flowed through the carbon felt, the flow visualization experiment produced a nearly flat front of the fluorescent dye (Figure 4). The behavior is consistent with plug flow, despite the low Reynolds number (Table 2:  $Re < 10$ ), suggesting that the carbon felt acted as an effective static mixer. This was the expected result, given that the diameter of the fibers of the felt were about  $20\ \mu\text{m}$  and thus much less than  $1/15^{\text{th}}$  the dimensions of the flow channel.<sup>39</sup> In the absence of the carbon felt, the fluid front was approximately parabolic (not shown), as would be expected for laminar flow in a rectangular channel.

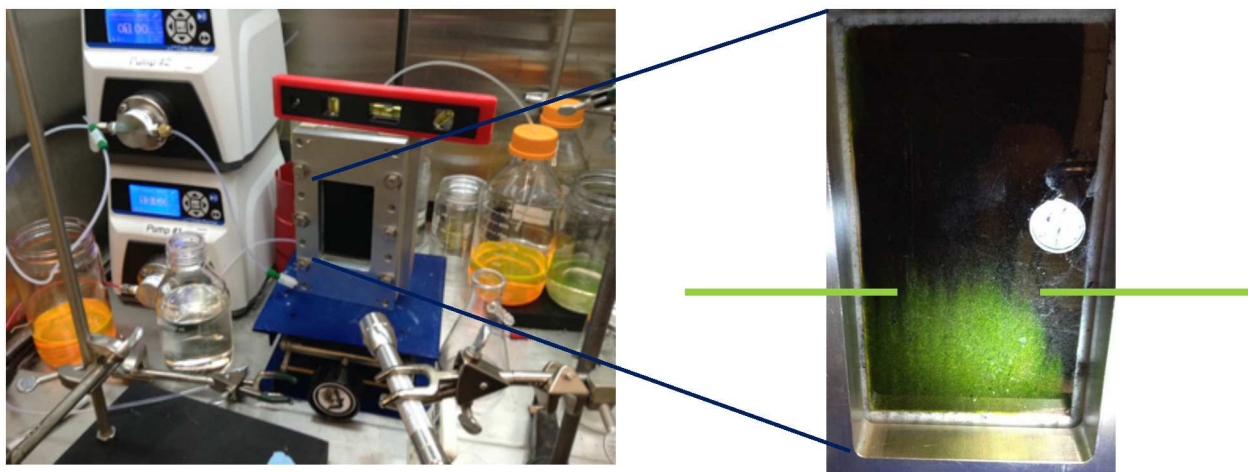


Figure 4. Visualization of flow in a the medium-sized electrolysis reactor at  $Re = 1.8$ .

**Residence time distribution.** We observed that the axial dispersion in the three reactors increased modestly with reactor size (~2-fold with a factor of 20-fold increase in reactor volume. Figure 5), which means that it should be possible to approximately maintain the residence time distribution while matching the mean residence times across scales of reactors.

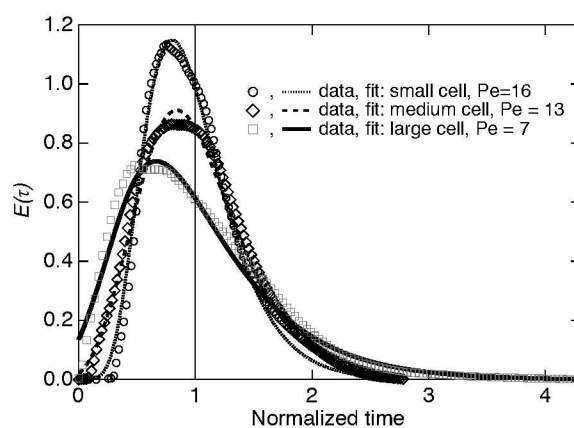


Figure 5. Normalized residence time distributions and their simulations for the three cells at similar hydraulic residence times: small cell (5 mL, 5.2 min), medium cell (29 mL, 5.9 min), large cell (100 mL, 4.8 min).

The trend in axial dispersion coefficient, (Figure 6), plausibly extrapolated to very low Reynolds numbers the results found by others for an electrolysis cell based on a much coarser, structured packing.<sup>40</sup>

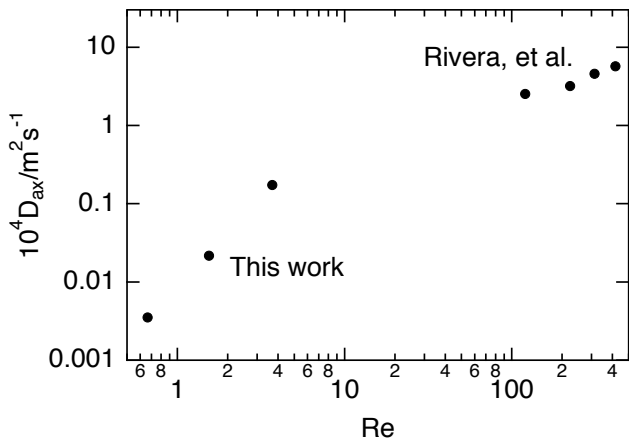


Figure 6. Comparison of axial dispersion in packed electrolysis cells. Results for  $Re > 100$  were reproduced from the work of Rivera, et al.<sup>40</sup>

**Mass transfer.** Flow around the fibers of the carbon felt promoted good transverse mixing, evidenced by the relation between axial dispersion and  $Re$  (Figure 6), and correspondingly good rates of mass transport (Figure 7), despite very low values of the Reynolds numbers.

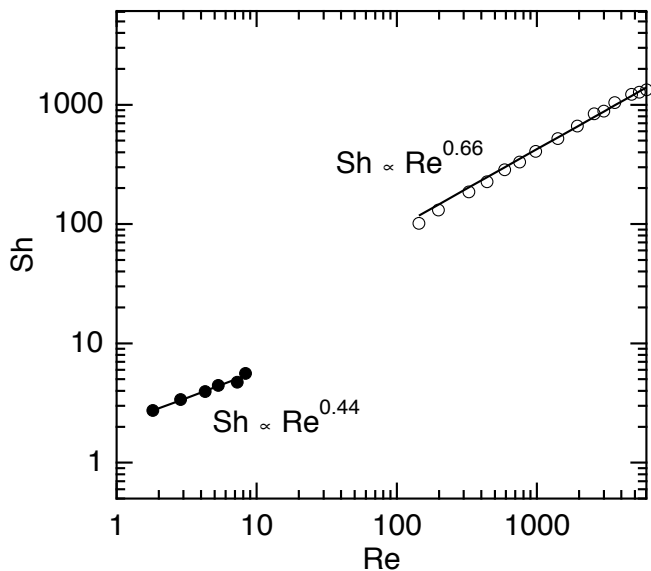


Figure 7. Mass transport through to/from the carbon felt as inferred from the transport-limited rates of reduction of ferricyanide. ●—this work; ○—Ralph, et al.<sup>37</sup>



**Reaction Kinetics.** The conversions,  $\chi$ , were modeled as first-order kinetics for the substrate reacting in a plug flow reactor (residence time,  $\tau$ ), with rate constants that depended on the applied overpotential,  $\eta$ , exchange current,  $k_0$ , the number of electrons transferred,  $z$ , a symmetry factor,  $\alpha$ , and the Faraday constant,  $F$ , through the Butler-Volmer relation (eq. 4):

$$\chi = \exp \left[ -k_0 \left( \exp \left( \frac{\alpha z F \eta}{RT} \right) - \exp \left( -\frac{1 - \alpha z F \eta}{RT} \right) \right) \tau \right] \quad \text{eq. 4}$$

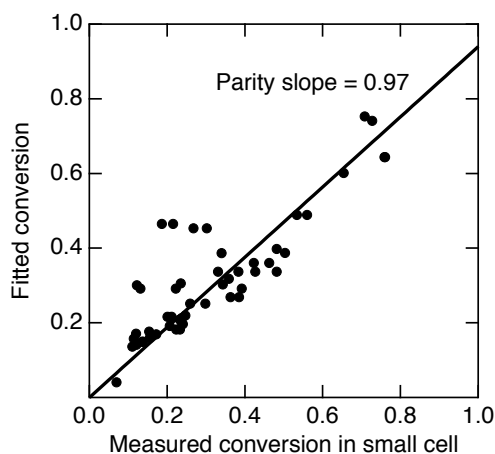


Figure 8. Parity plot between observed and fitted Butler-Volmer kinetics for the conversion of nitrobenzene at 25 °C, over ranges of residence time,  $\tau$ , cell potential,  $E_{cell}$ , inlet concentration,  $C_0$ , and loading,  $L$ , of Cu on the C support:  $150 < \tau/s < 450$ ,  $-1.5 < E_{cell}/V < -1.5$ ,  $0.05 < C_0/M < 0.253$ ,  $1\% < L/g_{Cu} \text{ gC}^{-1} < 4\%$ .

While the cell voltage is well defined, there could still be potential field gradients along and across the cell<sup>41</sup> leading to locally varying rates that are “mixing cup” averaged in the experiments reported in Figure 8. In experiments not reported here, we attempted to detect those gradients by inserting a micro reference electrode at several positions in the cell. The changes we observed were small and not obviously systematic. So, much like it is common to report a single reactor temperature even for highly exothermic or endothermic reactions we recognize the importance of, but have not quantified the details of, the potential field in the reactor (or even the

half-cell potentials). The field gradients will be strongest when the reactor is operated at high conversion.

*Hydrodeoxygenation of nitro arenes.* Both C-supported Cu and Fe catalysts proved competent for the hydrodeoxygenation of the nitro arenes, but Cu catalyst was more active (Figure 9).

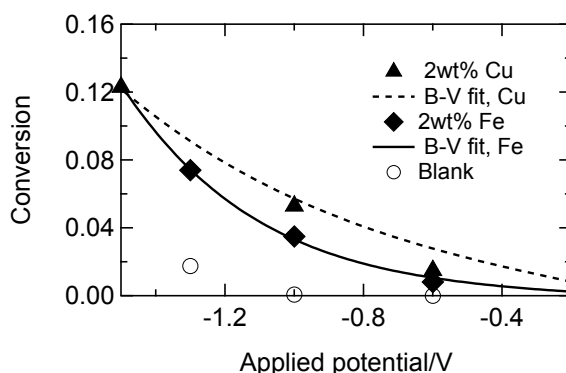


Figure 9. Electrochemical hydrodeoxygenation of nitrobenzene catalyzed by carbon-supported 2wt% Fe/C felt ( $\blacklozenge$ ), 2wt% Cu/C felt ( $\blacktriangle$ ) and bare felt ( $\circ$ ) electrodes. Inlet concentration of the substrate,  $C_0 = 20$  mM in the catholyte described in Table 4. Product selectivity = 100%.

*Effect of temperature.* We used the felt-supported iron and copper catalysts to probe the effect of changing the temperature of the electrolysis of methyl 3-nitrobenzoate (Figure 10). The results corresponded to an apparent activation energy of  $\sim 30$  kJ/mol.

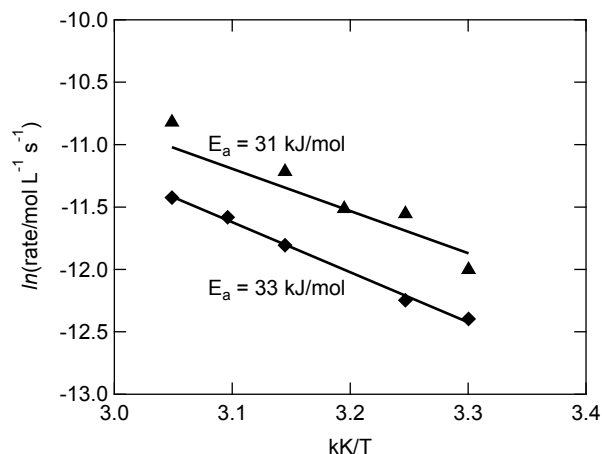


Figure 10. Effect of reaction temperature on the conversion of methyl 3-nitrobenzoate. Inlet concentration,  $C_0=40$  mM; Catalysts: 2 wt % Fe (♦) and 2wt% Cu (▲),  $E_{\text{cell}}=-1\text{V}$ , Residence time: 260 s.

*Effect of electrolyte.* The product slate in the electrochemical hydrodeoxygenation of methyl 3-nitrobenzoate could be narrowed to just the intended aniline by adjusting the pH of the catholyte and the applied cell potential (Figure S-1, bottom).

This substrate was sparingly soluble in the highly polar electrolyte. In preparation to contend with even less hydrophilic substrates, we tested the electrochemical hydrodeoxygenation of methyl 3-nitrobenzoate in an electrolyte containing a surfactant (Triton™ X-100) to learn whether the addition of the surfactant interfered with the electrolysis. Adding 30 g/L of surfactant (about twice its critical micelle concentration<sup>42</sup>) permitted us to approximately double the concentration of the substrate (from 0.04 mM to 0.092 mM) and did not inhibit the rate of conversion of the electrolysis reaction (Figure 11), leading to an effective doubling of the productivity of the reactor. However, the surfactant likely would complicate downstream separations.

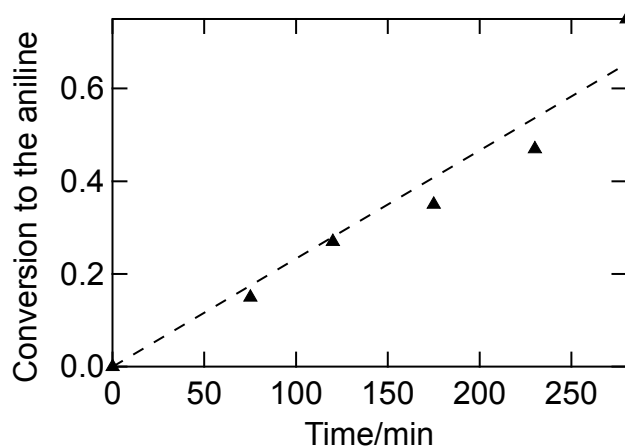


Figure 11. Effect of adding a surfactant to the electrolyte for the electrochemically activated conversion of methyl 3-nitrobenzoate to the corresponding aniline in a recirculating reactor. ▲ – 2 wt % Cu/C felt,  $E_{cell} = -1.3$  V,  $\tau = 206$  s,  $C_0 = 0.092$  M dissolved in the standard catholyte containing 30 g/L of Triton™ X-100; Dashed line: rate of conversion extrapolated from the steady state performance of the same catalyst operating in a plug flow reactor under the same conditions but using an electrolyte without the surfactant.

*Membrane-supported catalyst.* The differences between supporting the Cu catalyst on the membrane and on the graphite felt were modest (Figure 12). Yields were higher with the felt-supported catalyst at long contact times (low flow rates) because Cu/C felt was both more active and more selective. At shorter contact times, the activities converged, and the membrane-supported catalyst proved more selective. We have suggested how to make the felt-supported catalyst even more welcoming to the approach of hydrophobic molecules<sup>43</sup>: decorate the surface of the felt with pendant lipophiles. Even more subtle architecting has been discussed by others,<sup>44</sup> albeit for the surfaces of insulators.

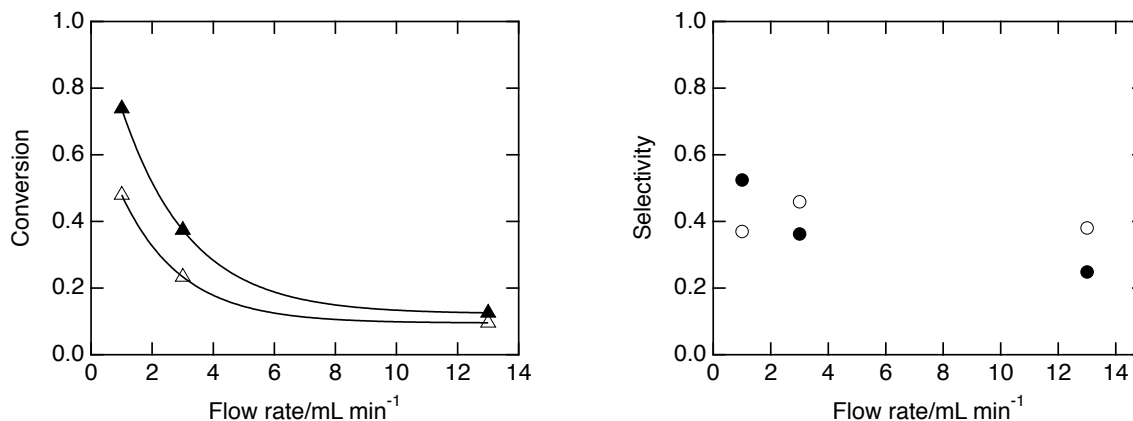


Figure 12. Comparison of hydrodeoxygenation of methyl 3-nitrobenzoate in the small cell (volume = 5 mL) of a membrane-supported Cu catalyst ( $\Delta$ - conversion,  $\circ$ - selectivity) with that of a felt-supported analog ( $\blacktriangle$ -conversion,  $\bullet$ -selectivity). Conditions: applied cell potential,  $E_{cell} = -0.5$  V, flow rate as indicated, inlet concentration of substrate,  $C_0 = 38$  mM. Solid lines are fits to first order kinetics,  $\chi = \exp(-k \tau)$ .

*Hydrodeoxygenation of 1-chloro-2-methyl-3-nitrobenzene.* In the reduction of this substrate, the Cu catalyst could be operated at significantly more cathodic potentials than a catalyst consisting of Pd/C felt (Figure 13, left). At the more negative potentials, the Pd catalyst produced large amounts of hydrogen, observed as bubbles in the effluent stream, which interfered with the reduction of the nitro arene. Even at less cathodic potentials, the Pd catalyst was active for a side-reaction, hydrodechlorination, as well as the hydrodeoxygenation of the -nitro group; the Cu catalyst was selective for just the desired hydrodeoxygenation. At higher potentials, the Cu catalyst continued to reduce the substrate and its current efficiency passed through a maximum (Figure 13, right). The production of either of the anilines (3-chloro-2-methylaniline or 2-methylaniline) were counted in the numerator of the current efficiencies shown in Figure 13.

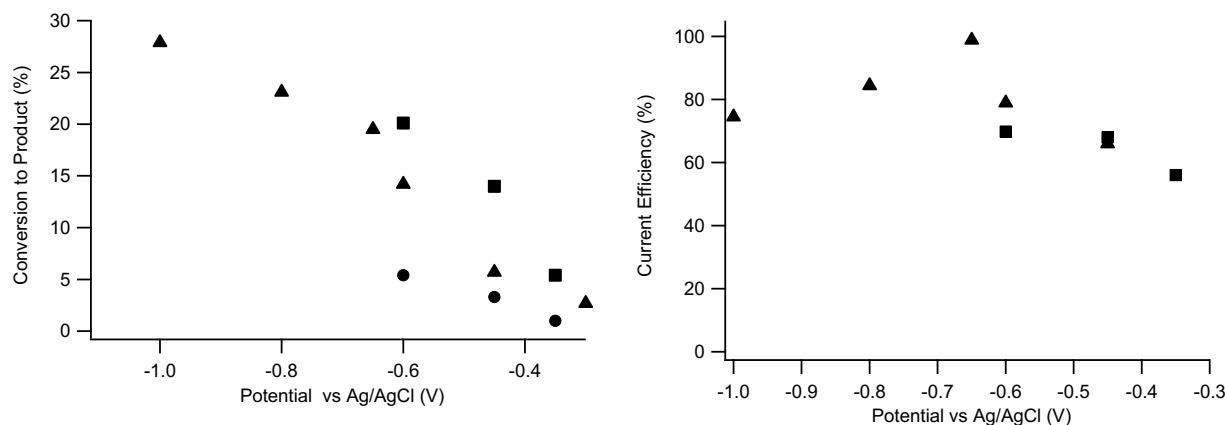


Figure 13. Comparison of activity (left) and current efficiency (right) of 4 wt% Cu/C felt and 4t% Pd/C felt for the hydrodeoxygenation of 1-chloro-2-methyl-3-nitrobenzene to 2-methyl-3-chloroaniline (▲-Cu; ■-Pd) and 2-methylaniline (●-Pd, none observed with the copper catalyst).

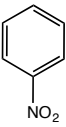
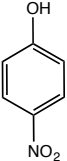
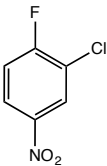
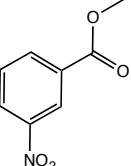
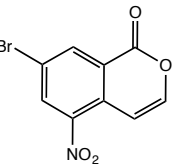
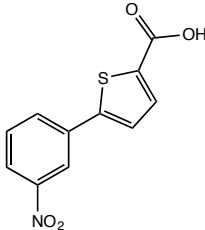
Conditions: the indicated half-cell potential of the cathode was referenced to a micro Ag/AgCl electrode (Harvard Apparatus) inserted in the cathode compartment, the residence times,  $\tau = 300$  s, the initial concentration of the substrate,  $C_0 = 37$  mM.

*Hydrodeoxygenation of 2-chloro-1-fluoro-4-nitrobenzene.* With tuning of the pH of the electrolyte, the applied voltage and the residence time, the copper catalyst proved active and selective (Figure S-2).

*Hydrodeoxygenation of 7-bromo-5-nitro-1H-isochromene-1-one.* Cu/C felt was again active and selective for the hydrodeoxygenation of the nitro group. However, in this case, the product rearranged (Figure S-3) in contact with the basic electrolyte (only 3% remained after 2 h of contact), implying the need for a rapid separation online separation/extraction to achieve high process yield.

*Hydrodeoxygenation of 4-nitrophenol and 5-(3-nitrophenyl)thiophene-2-carboxylic acid.* These substrates presented the challenge of regioselectivity—reducing the -nitro group in the presence of a carbonyl or hydroxyl—and self-inhibition—a sulfur moiety that would tend to poison a thermally activated, base-metal catalyst. While we did not study their reactions in detail,

we note that their conversions were in line with those of the other nitro arenes (Scheme 2). We noted but do not have an explanation for the interesting trend shown in Scheme 2 for the reactivity of these nitro arenes (inferred from their conversions under comparable conditions).

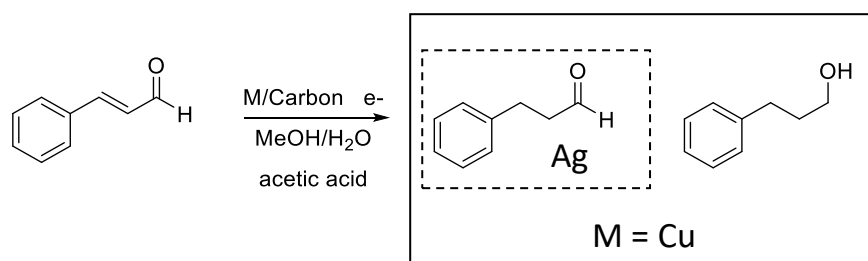
Substrate						
Conditions:						
Catalyst	Cu/C felt	Fe/C felt	Cu/C felt	Cu/C felt	Cu/C felt	Fe/C felt
$E_{cell}$	-1 V	-1 V	-1 V	-1 V	-1 V	-1 V
$\tau$	390 s	390 s	390 s	390 s	360 s	375 s
$C_0$	80 mM	80 mM	80 mM	40 mM	4 mM	7 mM
Conversion	5.3%	5%	5.4%	10.9%	~34%	50%
Selectivity	100%	100%	100%	100%	100%	100%

Scheme 2. Comparison of the electrochemical hydrodeoxygenation of the functionalized nitro arenes studied here.  $E_{cell}$ —applied cell potentials;  $\tau$ —residence times are based on 1 pass through the 6 mL flow reactor;  $C_0$ —inlet concentration. Selectivity refers to conversion of the substrate to the analogous amine.

*Hydrogenation of a nitrile.* We chose to use Co/C felt for this reaction because Co is known to be active for the hydrogenation<sup>45</sup> but has a higher overpotential against the evolution of H<sub>2</sub> than do the platinum group metals.<sup>46</sup> Therefore, it electrolyzes the water in the electrolyte more slowly and thus offers a higher current efficiency towards the desired product (the amine). We found a large effect of the cosolvent employed in the catholyte (Figure S-4): in methanol, there was a noticeable conversion of the benzonitrile to benzylamine (~5%); in tetrahydrofuran the conversion was much lower (<1%). We note that nitriles are reduced only at high temperature

and pressure ( $T > 150\text{ }^{\circ}\text{C}$ ;  $P > 3\text{ bar}$ ) when the reaction is carried out thermally using a Raney Co catalyst.<sup>45</sup>

*Hydrogenation of cinnamaldehyde.* We studied this reaction only qualitatively to survey the effect of different metals. Using the standard catholyte and an inlet concentration of the substrate of 30 mM, we found that 2 wt% Ag/Cu felt selectively hydrogenated the C=C double bond; at the same reaction conditions, 2 wt% Cu/C felt gave a mixture of olefin and carbonyl reduction (Scheme 3).



Scheme 3 Selectivity pattern in the electrochemically activated hydrogenation of cinnamaldehyde, using either 2 wt% Ag/C felt or 2 wt% Cu/C felt. Conditions:  $E_{cell} = -1.5\text{ V}$ ,  $\tau = 460\text{ s}$ ,  $C_0 = 38\text{ mM}$  substrate dissolved in the standard catholyte (MeOH:H<sub>2</sub>O (4:1) 5% acetic acid).

### Scale-up.

The same kinetics expression determined for the hydrodeoxygenation of nitrobenzene in the small cell applied to the reaction when it was carried in the medium-sized cell using catalysts from the same lot (Figure 14). That result was expected given the similar rheology of the cells (Figure 5).



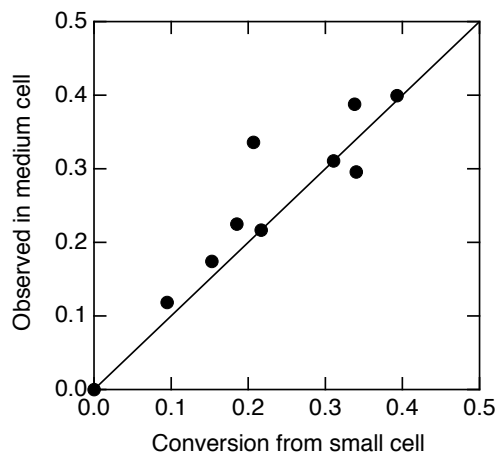


Figure 14. Parity plots of Butler-Volmer kinetics determined in the small cell for the conversion of nitrobenzene and then extrapolated to the medium sized cell using eq. 4; catalyst: 4 wt% Cu/C felt;  $0.05 < C_0/M < 0.253$ ;  $-1.1 < E_{\text{cell}}/V < -0.1$ ;  $150 < \tau/s < 450$ .

As a first step towards scaling, we ran a pair of the 27 mL reactors in parallel for 4 hours, each operating at an applied potential  $E_{\text{cell}} = -1.1$  V. Flowing an electrolyte solution containing 1-chloro-2-methyl-3-nitrobenzene (300 mM) through each cell at 5.4 mL/min (residence time = 300 s) produced a combined stream of 2.4 g/h of the aniline, corresponding to a conversion of 70% (analysis by GC). During the run, we observed no change in the current (2 A/cell). Linearly extrapolating those results suggests a production rate of 20 kg/y at the selected residence time. Therefore, a bank of 50 reactors, each roughly the size of a paperback book, or a proportionately smaller number of the larger reactors, could suffice to produce 500 kg/y of this product: because the reaction kinetics are approximately 1<sup>st</sup> order, conversion depends on the rate constant times residence time (reactor volume  $\div$  flow rate), regardless of how that volume is configured, provided that is equally accessible and active.

The catalysts did leach small quantities of metal during the long run. An aliquot of the product from early in the run contained 30 ppm Cu (ICP, Galbraith Labs) however aliquots from later in

the run showed a much lower accumulation of Cu in the product (0.79 ppm). Possibly, the earlier sampling corresponded to mechanical rather than chemical transport of Cu from the catalyst.

We note that we made no effort to stabilize the metals except to ensure that they were cathodically protected whenever they were in contact with the electrolyte.

## Conclusion

We chose to focus this foray into electrochemistry on the electrochemical reduction of nitro arenes because it is a class of reactions that has been known and studied for about 125 years,<sup>4</sup> albeit not as quantitatively or as reproducibly as we have tried to report here. Despite that long history, electrochemistry was not mentioned in a recent review<sup>47</sup> of routes to reducing aromatic - nitro groups. That absence implies that electrochemistry is not familiar or convenient to many process chemists and chemical engineers. Yet, the reactor geometry and catalysts described here are readily scalable<sup>48</sup> and tunable to achieve high selectivities, high rates and robust, continuous operation that enhances safety (by obviating the need for high pressure hydrogen) and that decreases the footprint of the unit operation (through the process intensification afforded by electrochemical activation of reaction intermediates).

We have shown that a suitable choice of catalyst can confer regioselectivity and resistance to interference by other chemical moieties. We have not discussed the promise of electrochemical oxidation either for direct conversion (adsorption of reactants, desorption of transformed products) or indirect conversion (generation of mediators) of valuable chemical products. We have also not discussed the required surround technologies (membranes, process analytical technology, process control, separations), nor the systematics of selection of the catalyst, electrolyte, or process conditions (residence time, applied voltage), all of which merit much more

1  
2  
3 attention. We note in passing that electrochemistry provides a direct, if modest,<sup>49</sup> way to “green”  
4  
5 the chemical process industry through the use renewably sourced power. In the past, electrons  
6  
7 were an expensive way to activate chemical processes, however, purchasing power agreements  
8  
9 for renewable power can lower the cost of electricity to less than \$0.03/kWh.<sup>50</sup>  
10  
11  
12  
13  
14

## 15 16 AUTHOR INFORMATION

17 Corresponding Author

18  
19 \*Robert.Weber@pnnl.gov  
20  
21  
22  
23

## 24 25 Funding Sources

26 This work was initiated under a Strategic Partnering Agreement between GSK and Pacific  
27  
28 Northwest National Laboratory (PNNL) and was completed with Laboratory Directed Research  
29  
30 and Development funding from PNNL. PNNL is a multi-program national laboratory operated  
31  
32 for the US Department of Energy by Battelle under contract DE-AC05-76RL01830  
33  
34  
35  
36  
37

## 38 39 ABBREVIATIONS

40 D diffusion coefficient,  $D_e$  effective diameter,  $L_c$  dimensionless length,  $Sc$  Schmidt number,  $Sh$   
41  
42 Sherwood Number,  $Re$  Reynolds Number,  $Pe$  Péclet number  
43  
44  
45  
46  
47

## 48 49 Supporting Information

50  
51 The supporting information is available free of charge on the ACS Publications website at DOI:  
52 10.1021/acs.oprd.xxxxxxx.  
53

54 It provides chromatographic and spectroscopic characterizations of the product mixtures to  
55 substantiate the discussion in the main article.  
56  
57  
58  
59  
60

## REFERENCES

- (1) Botte, G. G.; Daramola, D. A.; Muthuvel, M. *Preparative electrochemistry for organic synthesis*; Elsevier, 2014; Vol. 9.
- (2) Fry, A. J. *Synthetic Organic Chemistry*; Harper & Row: New York, 1972.
- (3) Walsh, F. C.; Ponce de León, C. *Electrochimica Acta*, Progress in electrochemical flow reactors for laboratory and pilot scale processing, **2018**, 280, 121-148, 10.1016/j.electacta.2018.05.027.
- (4) Lob, W. *Electrochemistry of Organic Compounds*; John Wiley&Sons: New York, 1906.
- (5) Yan, M.; Kawamata, Y.; Baran, P. S. *Angew Chem Int Ed Engl*, Synthetic Organic Electrochemistry: Calling All Engineers, **2017**, 57, 4149-4155, 10.1002/anie.201707584.
- (6) Lund, H. J. *Electrochem. Soc.*, A Century of Organic Electrochemistry, **2002**, 149, S21-S33.
- (7) Wiebe, A.; Gieshoff, T.; Mohle, S.; Rodrigo, E.; Zirbes, M.; Waldvogel, S. R. *Angew Chem Int Ed Engl*, Electrifying Organic Synthesis, **2018**, 57, 5594-5619, 10.1002/anie.201711060.
- (8) Frontana-Uribe, B. A.; Little, R. D.; Ibanez, J. G.; Palma, A.; Vasquez-Medrano, R. *Green Chemistry*, Organic electrosynthesis: a promising green methodology in organic chemistry, **2010**, 12, 2099-2119.
- (9) Francke, R.; Little, R. D. *Chem Soc Rev*, Redox catalysis in organic electrosynthesis: basic principles and recent developments, **2014**, 43, 2492-2521.
- (10) Möhle, S.; Zirbes, M.; Rodrigo, E.; Gieshoff, T.; Wiebe, A.; Waldvogel, S. R. *Angewandte Chemie International Edition*, Modern Electrochemical Aspects for the Synthesis of Value-Added Organic Products, **2018**, 57, 6018-6041, 10.1002/anie.201712732.
- (11) Vaze, A. S.; Sawant, S. B.; Pangarkar, V. G. *J. Appl. Electrochem.*, Electrochemical oxidation of isobutanol to isobutyric acid in a flow cell, **1995**, 25, 279-283.
- (12) Ika, 2018, Electrosyn flow, <https://www.ikaprocess.com/en/Products/Custom-products-cph-45/ElectraSyn-flow-csb-ES/>, accessed on: 3 August 2018.
- (13) CTech Innovation, 2018, Electrochemical Synthesis, <http://www.ctechinnovation.com/electrochemical-synthesis/>, accessed on:
- (14) The Fuel Cell Store, 2018, Expandable PEM Research Test Cell - 50cm<sup>2</sup>, <http://www.fuelcellstore.com/expandable-pem-research-test-cell-50cm>, accessed on: 3 August 2018.
- (15) Scott, K. *Electrochemical Processes for Clean Technology*; Royal Society of Chemistry: Cambridge, 1995.
- (16) Bernasconi, E.; Genders, D.; Lee, J.; Longoni, D.; Martin, C. R.; Menon, V.; Roletto, J.; Sogli, L.; Walker, D.; Zappi, G.; Zelenay, P.; Zhang, H. *Org. Process Res. Dev.*, Ceftibuten:Development of a Commercial Process Based on Cephalosporin C. Part II. Process for the Manufacture of 3-Exomethylene-7(R)-glutaroilaminocepham-4-carboxylic Acid 1(S)-Oxide, **2002**, 6, 158-168, 10.1021/op0100706.
- (17) Chai, D.; Genders, D.; Weinberg, N.; Zappi, G.; Bernasconi, E.; Lee, J.; Roletto, J.; Sogli, L.; Walker, D.; Martin, C. R.; Menon, V.; Zelenay, P.; Zhang, H. *Org. Process Res. Dev.*, Ceftibuten:Development of a Commercial Process Based on Cephalosporin C. Part IV. Pilot-Plant Scale Electrochemical Reduction of 3-Acetoxymethyl-7(R)-

- glutarylaminocyclohexanecarboxylic Acid 1(S)-Oxide, **2002**, *6*, 178-183, 10.1021/op010072q.
- (18) Degenring, D.; Schroeder, I.; Wandrey, C.; Liese, A.; Greiner, L. *Org. Process Res. Dev.*, Resolution of 1,2-Diols by Enzyme-Catalyzed Oxidation with Anodic, Mediated Cofactor Regeneration in the Extractive Membrane Reactor: Gaining Insight by Adaptive Simulation, **2004**, *8*, 213-218, 10.1021/op034122y.
- (19) Muzumdar, A. V.; Sawant, S. B.; Pangarkar, V. G. *Org. Process Res. Dev.*, Reduction of Maleic Acid to Succinic Acid on Titanium Cathode, **2004**, *8*, 685-688, 10.1021/op0300185.
- (20) Cai, W.; Colony, J. L.; Frost, H.; Hudspeth, J. P.; Kendall, P. M.; Krishnan, A. M.; Makowski, T.; Mazur, D. J.; Phillips, J.; Ripin, D. H. B.; Ruggeri, S. G.; Stearns, J. F.; White, T. D. *Org. Process Res. Dev.*, Investigation of Practical Routes for the Kilogram-Scale Production of cis-3-Methylamino-4-methylpiperidines, **2005**, *9*, 51-56, 10.1021/op049808k.
- (21) Kataoka, K.; Hagiwara, Y.; Midorikawa, K.; Suga, S.; Yoshida, J.-i. *Org. Process Res. Dev.*, Practical Electrochemical Iodination of Aromatic Compounds, **2008**, *12*, 1130-1136, 10.1021/op800155m.
- (22) Arai, K.; Wirth, T. *Org. Process Res. Dev.*, Rapid Electrochemical Deprotection of the Isonicotinylcarbonyl Group from Carbonates and Thiocarbonates in a Microfluidic Reactor, **2014**, *18*, 1377-1381, 10.1021/op500155f.
- (23) Green, R. A.; Brown, R. C. D.; Pletcher, D.; Harji, B. *Org. Process Res. Dev.*, A Microflow Electrolysis Cell for Laboratory Synthesis on the Multigram Scale, **2015**, *19*, 1424-1427, 10.1021/acs.oprd.5b00260.
- (24) Gütz, C.; Baenziger, M.; Bucher, C.; Galvao, T. R.; Waldvogel, S. R. *Org. Process Res. Dev.*, Development and Scale-Up of the Electrochemical Dehalogenation for the Synthesis of a Key Intermediate for NS5A Inhibitors, **2015**, *19*, 1428-1433, 10.1021/acs.oprd.5b00272.
- (25) Gütz, C.; Kloeckner, B.; Waldvogel, S. R. *Org. Process Res. Dev.*, Electrochemical Screening for Electroorganic Synthesis, **2016**, *20*, 26-32, 10.1021/acs.oprd.5b00377.
- (26) Shi, C.; Chan, K.; Yoo, J. S.; Nørskov, J. K. *Organic Process Research & Development*, Barriers of Electrochemical CO<sub>2</sub> Reduction on Transition Metals, **2016**, *20*, 1424-1430, 10.1021/acs.oprd.6b00103.
- (27) Gütz, C.; Stenglein, A.; Waldvogel, S. R. *Org. Process Res. Dev.*, Highly Modular Flow Cell for Electroorganic Synthesis, **2017**, *21*, 771-778, 10.1021/acs.oprd.7b00123.
- (28) Karimi, B.; Ghahremani, M.; Ciriminna, R.; Pagliaro, M. *Organic Process Research & Development*, New Stable Catalytic Electrodes Functionalized with TEMPO for the Waste-Free Oxidation of Alcohol, **2018**, *22*, 1298-1305, 10.1021/acs.oprd.8b00156.
- (29) Sanyal, U.; Lopez-Ruiz, J.; Padmaperuma, A. B.; Holladay, J.; Gutiérrez, O. Y. *Organic Process Research & Development*, Electrocatalytic Hydrogenation of Oxygenated Compounds in Aqueous Phase, **2018**, 10.1021/acs.oprd.8b00236.
- (30) Cao, Y.; Noel, T. *Org. Process Res. Dev.*, Efficient Electrocatalytic Reduction of Furfural to Furfuryl Alcohol in a Microchannel Flow Reactor, **2019**, *23*, 403-408, 10.1021/acs.oprd.8b00428.
- (31) Yang, Z. G., 2017, It's Big and Long-Lived, and It Won't Catch Fire: The Vanadium Redox-Flow Battery, <https://spectrum.ieee.org/green-tech/fuel-cells/its-big-and->

- [longlived-and-it-wont-catch-fire-the-vanadium-redoxflow-battery](#), accessed on: 3 August 2018.
- (32) Kim, S.; Thomsen, E.; Xia, G.; Nie, Z.; Bao, J.; Recknagle, K.; Wang, W.; Viswanathan, V.; Luo, Q.; Wei, X.; Crawford, A.; Coffey, G.; Maupin, G.; Sprenkle, V. *Journal of Power Sources*, 1 kW/1 kWh advanced vanadium redox flow battery utilizing mixed acid electrolytes, **2013**, 237, 300-309, 10.1016/j.jpowsour.2013.02.045.
- (33) Lopez-Ruiz, J. A.; Sanyal, U.; Egbert, J.; Gutiérrez, O. Y.; Holladay, J. *ACS Sustainable Chemistry & Engineering*, Kinetic Investigation of the Sustainable Electrocatalytic Hydrogenation of Benzaldehyde on Pd/C: Effect of Electrolyte Composition and Half-Cell Potentials, **2018**, 6, 16073-16085, 10.1021/acssuschemeng.8b02637.
- (34) Kendrick, I.; Smotkin, E. S. *International Journal of Hydrogen Energy*, Operando infrared spectroscopy of the fuel cell membrane electrode assembly Nafion-platinum interface, **2014**, 39, 2751-2755, 10.1016/j.ijhydene.2013.07.117.
- (35) Davis, M. E.; Davis, R. J. *Fundamentals of chemical reaction engineering*; McGraw-Hill: New York, 2003.
- (36) Mathworks, 2016, Matlab R2106b.
- (37) Ralph, T. R.; Hitchman, M. L.; Millington, J. P.; Walsh, F. C. *Electrochim Acta*, Mass transport in an Electrochemical Laboratory Filterpress reactor and its Enhancement by Turbulence Promoters, **1996**, 41, 591-603.
- (38) Konopka, S. J.; McFuffie, B. *Anal. Chem.*, Diffusion coefficients of ferri- and ferrocyanide ions in aqueous media, using twin-electrod thin-layer electrochemistry, **1970**, 42, 1741-1746.
- (39) Stahel, E. P.; Geankoplis, C. J. *AIChE J*, Axial diffusion and pressure drop of liquids in porous media, **1964**, 10, 174-179.
- (40) Rivera, F. F.; Cruz-Díaz, M. R.; Rivero, E. P.; González, I. *Electrochimica Acta*, Analysis and interpretation of residence time distribution experimental curves in FM01-LC reactor using axial dispersion and plug dispersion exchange models with closed-closed boundary conditions, **2010**, 56, 361-371, 10.1016/j.electacta.2010.08.069.
- (41) Shah, A. A.; Luo, K. H.; Ralph, T. R.; Walsh, F. C. *Electrochimica Acta*, Recent trends and developments in polymer electrolyte membrane fuel cell modelling, **2011**, 56, 3731-3757, 10.1016/j.electacta.2010.10.046.
- (42) Tiller, G. E.; Mueller, T. J.; Dockter, M. E.; Struve, W. G. *Anal Biochem*, Hydrogenation of Triton X-100 Eliminates Its Fluorescence and Ultraviolet Light Absorption while Preserving Its Detergent Properties, **1984**, 141, 262-266.
- (43) Cantu, D. C.; Wang, Y.-G.; Yoon, Y.; Glezakou, V.-A.; Rousseau, R.; Weber, R. S. *Catalysis Today*, Heterogeneous catalysis in complex, condensed reaction media, **2017**, 289, 231-236, 10.1016/j.cattod.2016.08.025.
- (44) Brunelli, N. A.; Venkatasubbaiah, K.; Jones, C. W. *Chemistry of Materials*, Cooperative Catalysis with Acid-Base Bifunctional Mesoporous Silica: Impact of Grafting and Co-condensation Synthesis Methods on Material Structure and Catalytic Properties, **2012**, 24, 2433-2442, 10.1021/cm300753z.
- (45) Dai, C.; Zhu, S.; Wang, X.; Zhang, C.; Zhang, W.; Li, Y.; Ning, C. *New Journal of Chemistry*, Efficient and selective hydrogenation of benzonitrile to benzylamine: improvement on catalytic performance and stability in a trickle-bed reactor, **2017**, 41, 3758-3765, 10.1039/c7nj00001d.

- (46) Trassati, S. J. *Electroanal. Chem.*, Work Function, Electronegativity, and Electrochemical Behaviour of metals III. Electrolytic Hydrogen Evolution in Acid Solutions., **1972**, 39, 163-184.
- (47) Orlandi, M.; Brenna, D.; Harms, R.; Jost, S.; Benaglia, M. *Organic Process Research & Development*, Recent Developments in the Reduction of Aromatic and Aliphatic Nitro Compounds to Amines, **2018**, 22, 430-445, 10.1021/acs.oprd.6b00205.
- (48) Rivera, F. F.; Ponce de León, C.; Walsh, F. C.; Nava, J. L. *Electrochimica Acta*, The reaction environment in a filter-press laboratory reactor: the FM01-LC flow cell, **2015**, 161, 436-452, 10.1016/j.electacta.2015.02.161.
- (49) US Department of Energy, 2015, Bandwidth study on energy use and potential energy saving opportunities in US Chemical Manufacturing, <https://www.energy.gov/eere/amo/downloads/bandwidth-study-us-chemical-manufacturing>, accessed on:
- (50) US EPA, 2018, Green Power Pricing, <https://www.epa.gov/greenpower/green-power-pricing#fn2>, accessed on: 10 June 2018.